

REPORT DOCUMENTATION PAGE

Form Approved OMB No. 0704-0188

Public reporting burden for this collection of information is estimated to average 1 hour per response, including the time for reviewing instructions, searching existing data sources, gathering and maintaining the data needed, and completing and reviewing the collection of information. Send comments regarding this burden estimate or any other aspect of this collection of information, including suggestions for reducing the burden, to Department of Defense, Washington Headquarters Services, Directorate for Information Operations and Reports (0704-0188), 1215 Jefferson Davis Highway, Suite 1204, Arlington, VA 22202-4302. Respondents should be aware that notwithstanding any other provision of law, no person shall be subject to any penalty for failing to comply with a collection of information if it does not display a currently valid OMB control number.

PLEASE DO NOT RETURN YOUR FORM TO THE ABOVE ADDRESS.

1. REPORT DATE (DD-MM-YYYY) 26-09-2006	2. REPORT TYPE Final Report	3. DATES COVERED (From – To) 25 February 2005 - 25-Feb-06
--	---------------------------------------	---

4. TITLE AND SUBTITLE Slip Activity in Commercial Purity Titanium (CP Ti)	5a. CONTRACT NUMBER FA8655-05-1-3004
	5b. GRANT NUMBER
	5c. PROGRAM ELEMENT NUMBER

6. AUTHOR(S) Professor Tamas H Ungar	5d. PROJECT NUMBER
	5d. TASK NUMBER
	5e. WORK UNIT NUMBER

7. PERFORMING ORGANIZATION NAME(S) AND ADDRESS(ES) Eotvos University Budapest Pazmany Peter setany 1/A Budapest H-1117 Hungary	8. PERFORMING ORGANIZATION REPORT NUMBER N/A
---	--

9. SPONSORING/MONITORING AGENCY NAME(S) AND ADDRESS(ES) EOARD PSC 821 BOX 14 FPO AE 09421-0014	10. SPONSOR/MONITOR'S ACRONYM(S)
	11. SPONSOR/MONITOR'S REPORT NUMBER(S) Grant 05-3004

12. DISTRIBUTION/AVAILABILITY STATEMENT
Approved for public release; distribution is unlimited. (approval given by local Public Affairs Office)

13. SUPPLEMENTARY NOTES

14. ABSTRACT

This report results from a contract tasking Eotvos University Budapest as follows: The knowledge of the dislocation structure of Commercial Purity Titanium (CP Ti) in terms of dislocation densities and Burgers vector types and the twin- and stacking-fault densities in CP Ti are crucial for the following two reasons. (i) The knowledge of actual slip mechanisms controlling the plastic deformation of titanium determine its behaviour during processes involving plastic deformation. (ii) The brittle or ductile behaviour of a workpiece made of titanium depends on the content of the density and type of dislocations as well as the content of the twin- and stacking-fault densities. The aim of this research project is to determine the dislocation type and density and the twin- and stacking-fault densities in titanium specimens prepared by well defined plastic deformation procedures.

15. SUBJECT TERMS
EOARD, titanium alloys, Texture, Surface Processes

16. SECURITY CLASSIFICATION OF:			17. LIMITATION OF ABSTRACT UL	18, NUMBER OF PAGES 19	19a. NAME OF RESPONSIBLE PERSON KEVIN J LAROCHELLE, Maj, USAF
a. REPORT UNCLAS	b. ABSTRACT UNCLAS	c. THIS PAGE UNCLAS			19b. TELEPHONE NUMBER (Include area code) +44 (0)20 7514 3154

Final Fourth Delivery on the
Miniproject EOARD
20 September, 2006

title:

"Slip Activity in Commercial Purity Titanium (CP Ti)"

A joint scientific collaboration between

The Metals Processing Group of Dr Lee Semiatin
at the AF Research Laboratory in WPAFB, OH

and

The Diffraction Group of Professor Dr Tamás Ungár
at the Department of General Physics of the Eötvös University Budapest in Hungary

A. Introduction/Abstract

A/1. In the first delivery the microstructure of the CP-Ti specimen provided by The Metals Processing Group of Dr Lee Semiatin at the AF Research Laboratory in WPAFB, OH (in the following: AF-Partner) was determined by X-ray line profile analysis (XLPA).

A/2. In the second delivery cube specimens were prepared from the as received specimen, as shown schematically in Fig. 1 in the second report. The cubes were deformed by the method of *abc* deformation, i.e. the cubes were compressed successively on the *xx*, *yy* and *zz* surfaces to the same extent, respectively. Deformation was carried out to 10 and 20 % compression on each surface consecutively.

A/3. In the third deliverable the following were reported:

- (i) the orientation and diffraction on a single grain specimen, prepared by the method of focused ion beam (FIB), was carried out,
- (ii) the calculation of the effect of twinning on the $(10\bar{1}1)$ plane on the broadening of diffraction patterns was initiated,
- (iii) the preparation of thin rod-specimens for the purpose of high resolution single grain diffraction experiments in a special synchrotron experiment was described,
- (iv) home laboratory experiments on the small rod-specimens were presented,
- (v) qualitative comparison of measured and calculated twin-broadened powder patterns were presented,
- (vi) typical, first diffraction patterns of single grains in the synchrotron measurements were shown.

A/4. In the present, final report a summary of the work done during this grant period, is presented.

B. CP-Ti samples investigated

The CP-Ti specimen provided by The Metals Processing Group of Dr Lee Semiatin at the AF Research Laboratory in WPAFB, OH was a wrought block of dimensions of 50x40x30 mm. About 12 smaller cubes of about 6x6x6 mm dimensions were cut from the material by a diamond saw. Two deformation states were produced by the method of *abc* deformation, where the deformation stage was 10 and 20 % respectively. In the following the three specimens are called: initial state, 10 % deformed and 20 % deformed, respectively.

C. X-ray diffraction experiments in the home laboratory

Four different kinds of X-ray diffraction experiments were carried out. (i) Conventional θ - 2θ diffraction experiments in an Philips X'Pert diffractometer, (ii) diffraction experiments in a special high resolution diffractometer with negligible instrumental effect, using imaging plates as signal detectors, (iii) microdiffraction experiments on a single grain specimen, and (iv) first synchrotron experiments in a novel geometry with the novel purpose to extract single crystal data from polycrystalline specimens.

C/1. Conventional θ - 2θ diffraction experiments

The small cube specimen has been measured on all three perpendicular surfaces in order to see if there is considerable texture in the metal. The diffraction pattern corresponding to the *xx* surface, the surface perpendicular to the rolling direction, is shown in Fig. 1a in linear and Fig. 1b in logarithmic intensity scales, respectively. The diffraction patterns corresponding to the other two surfaces of the cube were almost identical to the one shown in Fig. 1, indicating no strong texture in the metal piece. The measured diffraction patterns (open circles) were evaluated by the convolutional multiple whole profile (CMWP) fitting procedure, cf. [1-4].

C/2. High resolution diffractometer measurements with imaging-plate (ip) signal detection

The full widths at half maximum (FWHM) of the first few reflections in a Williamson-Hall plot of the initial state specimen are shown in Fig. 2. *xx*, *yy* and *zz* correspond to the three surfaces of the cube specimen and $K=2\sin\theta/\lambda$, where θ is the diffraction angle and λ the wavelength of X-rays. The similar FWHM values in the three perpendicular directions indicate that there is no strong texture in the metal piece, in agreement with the measurements discussed in C/1.

The diffraction patterns obtained from the imaging plate measurements were first evaluated qualitatively in Williamson-Hall plots. The FWHM values of the three specimens are plotted in Williamson-Hall plots as a function of the diffraction vector, $K=2\sin\theta/\lambda$, in Fig. 3. The following can be observed from the figure. (i) In the initial state the material is practically strain free, i.e. the FWHM values are lying more or less along a horizontal line. The apparent scattering of the FWHM data is most probably due to the effect of twinning. (ii) In the deformed specimens the FWHM values show a global increasing trend with K , indicating the presence of microstrain. (iii) The microstrains are larger in the more deformed state. (iv) Strain anisotropy, i.e. the apparent scattering of the FWHM values can be observed, especially around $K=4$ and 8 , respectively.

Typical imaging plate (ip) readouts for the initial state (a) and the 20 % deformed (b) specimens in the higher diffraction angle range from about 60 to 120 degrees in 2θ are shown in Figs. 4. The following qualitative features can be seen in these figures. (1) Some of the Debye-Scherrer rings corresponding to the initial state specimen (a) are spotty, indicating that in this state of the material microstrains are small. This is in good correlation with the small values of the dislocation density determined from the quantitative evaluation and with the small slope in the Williamson-Hall plot. (2) The Debye-Scherrer rings corresponding to the 20 % deformed specimen (b) are perfectly smooth and strongly broadened compared to the initial state specimen. This indicates that the *abc* type deformation introduces a large amount of microstrains and that the microstructure becomes homogeneous.

The software developed for the correct integration of the intensity along the iso- 2θ lines in the plane of the imaging plates enables the determination of the θ - 2θ diffraction pattern. The diffraction patterns obtained by this integration procedure are shown in Figs. 5. It can be seen in a qualitative manner that in the initial state the peak profiles are rather narrow, note the logarithmic intensity scale. The profiles broaden successfully with deformation, as it can be seen in the other two patterns. The apparent variation of the FWHM values in Figs. 2 and 3 in

the initial state specimen are most probably due to twinning and not due to dislocations. The dislocation density and the fractions of the active slip system type have been determined successfully in the case of the two deformed specimens. The results are summarized in Tables 1 and 2.

Table 1. The median and variance, m and σ of the log-normal size distribution function, the area average mean subgrain size, $\langle x \rangle_{\text{area}}$, the dislocation density and arrangement parameters, ρ and M , as provided by the CMWP procedure.

Specimen	m [nm]	σ	$\langle x \rangle_{\text{area}}$ [nm]	ρ [10^{14} m^{-2}]	M
10 % Deformed	32 (5)	0.5 (0.1)	60 (10)	5.5 (2)	5 (2)
20 % Deformed	44 (5)	0.2 (0.05)	50 (10)	25 (5)	5 (2)

Table 2. The q_1 and q_2 parameters for strain anisotropy, and the fractions of the active slip system types, \bar{h}_a , \bar{h}_c and \bar{h}_{c+a} , as provided by the CMWP procedure and evaluated as described in detail in the first report (first deliverable).

Specimen	q_1	q_2	\bar{h}_a	\bar{h}_c	\bar{h}_{c+a}
10 % Deformed	0.12 (0.02)	0.45 (0.05)	0.65 (0.1)	0.35 (0.1)	0.0 (0.1)
20 % Deformed	-0.87 (0.05)	-0.07 (0.02)	0.85 (0.1)	0.15 (0.1)	0.0 (0.1)

C/3. Orientation and diffraction carried out on a single grain specimen prepared by the method of focused ion beam (FIB) in the AF Research Laboratory

A single grain from a forged CP-Ti bar was prepared by the method of focused ion beam in the AF Research Laboratory. The scanning electron microscopy (SEM) micrograph of the grain can be seen in Fig. 6a. The longer and shorter diameters of the grain are about 100 and 50 μm , respectively. The specimen was mounted on a glass rod and into a goniometer head in the Eulerian circle of the diffractometer. The specimen has been monitored by a small sharpness depth microscope attached to a digital camera and a TV monitor. The, about 25 times magnified image of the specimen can be seen in Fig. 6b. The bulging white spot is the image of the synthetic glue holding the grain, the dark contrast at the upper end of the glue is the single grain.

The orientation was attempted to be determined by a Laue diffractogram shown in Fig. 7a. A number of single diffraction spots can be seen in the Laue diffractogram, which were attempted to be indexed for hkl s. The diffraction image of the single grain specimen taken in the diffractometer by turning the specimen over the ω axis by about 10 degrees is shown in Fig. 7b. Three 10.1 type reflections can be seen on the image plate record, indicated by red arrows and the hkl indices. The curvatures, along which the diffraction spots are aligned, correspond to the Debye-Scherrer rings. The three 10.1 type reflections are as close to each other as about 10 and 15 degrees, respectively. Taking into account that the possible 10.1 reflections, stemming from a single crystal, cannot be closer to each other than 30 degrees, the appearance of three 10.1 reflections, when turning the crystal only by 10 degrees over the ω axis, indicates that the specimen must consist of more than just one single crystallite. It is possible that the upper layer of the single grain prepared by the method of FIB is a single crystallite, however, the entire specimen contains one or two additional crystallites. It is conceivable that the additional crystallites are in the deeper part of the specimen, which was not possible to be tested by the electron beam technique.

D. Preparation of small-rod specimens for the purpose of high resolution single grain diffraction experiments in a special synchrotron experiment

The special high resolution diffractometer, described in more detail in the first and second deliverable, works on the basis of parallel beam geometry, with a beam size at the specimen of about $100 \times 500 \mu\text{m}$. In order to eliminate the geometrical errors caused by large flat specimen surfaces, it was decided to prepare thin rods of diameters of about $500 \mu\text{m}$ and lengths between 4 and 8 mm. The specimens, used further in the synchrotron experiments were thinned down to diameters of about 100 to $200 \mu\text{m}$. In the home laboratory experiments the thin rods were mounted on a goniometer head which was placed into an Eulerian cradle.

D/1. Home laboratory experiments on the thin-rod specimens

Typical diffraction patterns corresponding to the thin rod specimens are shown in Fig. 8. The first three peaks, 100, 002 and 101 corresponding to the as received and 20 % deformed specimen are shown in logarithmic intensity scale in Fig. 8a. The back reflection parts of the same patterns are shown in Fig. 8b in linear intensity scales. The peaks are considerably broadened in the case of the deformed specimen, especially in the back reflection part of the pattern. It is worth to note that the abc deformation mode has strongly reduced the texture of the as received specimen. E.g., the 002 and 004 reflections in the as received specimen are very weak, whereas they become strong in the abc deformed specimen.

D/2. Typical diffraction patterns of single grains measured by a special synchrotron technique

The thin-rod specimens were measured in a special and novel synchrotron experimental technique very recently. The specimens are hit by a small focused X-ray beam of about $20 \mu\text{m}$ diameter and extremely small divergence. The scattered radiation is detected by a high

resolution area detector of 50 μm pixel size and 100x100 mm opening at a distance from the specimen at 200 mm in the close, and 700 mm in the high resolution diffraction mode, respectively. The specimen is rotated over the ω axis by $\Delta\omega$ steps of 0.2° and 0.5° over $\pm 60^\circ$ in the close and the high resolution diffraction modes, respectively. At each ω setting the diffraction pattern is measured for 8 seconds, and the pattern is stored. By this method 240 and 600 frames are stored in the close and the high resolution diffraction modes, respectively. Two typical close frames are shown in Figs. 9a and 9b, corresponding to the as received specimen. Each dark contrast on the image corresponds to an individual crystallite in the specimen. It can be seen that the intensity distributions are strongly elongated along the Debye-Scherrer ring directions indicating the presence of microstrains. This elongation is the so called rocking-curve broadening. The diffraction spots are less broad in the radial direction. This is a typical anisotropy of line broadening in plastically deformed materials. Some 300 frames were summed up and the resultant pattern is shown in Fig. 9c. Along the innermost ring a well developed six fold symmetry of the diffraction spots indicates a texture of the specimen. It is important to note that, in the case of the present figure, one diffraction spot corresponds to a large number of individual grains, or a large number of spots on the individual frames. A typical readout of an individual frame in the high resolution mode, i.e. at a 700 mm detector to specimen distance, is shown in Fig. 9d. Here it can be seen that the resolution is good enough for the evaluation of line broadening in the radial direction. The evaluation of the synchrotron experiments is in progress.

E. An abstract, based on the present work, has been submitted to the TMS meeting:

"Structural Materials Division Symposium: Mechanical Behavior of Nanostructured Materials, in honor of Carl Koch"

2007 TMS Annual Meeting, February 25-March 1, Orlando, FL

In the full length article due for the proceedings of the symposium the grant will be duly acknowledged.

Acknowledgement of Sponsorship: I am responsible for assuring that an acknowledgement of Government support will appear in any publication of any material based on or developed under this project, in the following terms: "Effort sponsored by the Air Force Office of Scientific Research, Air Force Material Command, USAF, under grant number FA8655-05-1-3004. The U.S. Government is authorized to reproduce and distribute reprints for Government purpose notwithstanding any copyright notation thereon."

I am responsible for assuring that every publication of material based on or developed under this project contains the following disclaimer: "The views and conclusions contained herein are those of the author and should not be interpreted as necessarily representing the official policies or endorsements, either expressed or implied, of the Air Force Office of Scientific Research or the U.S. Government."

I certify that there were no subject inventions to declare during the performance of this grant.

The Use of X-Ray Diffraction to Determine Slip and Twinning Activity in Commercial-Purity (CP) Titanium

T. Ungár¹, K. Nyilas¹, M. Glavicic^{2,3}, L. Balogh¹, A. A. Salem^{2,4},
and S. L. Semiatin²

¹Department Materials Physics, Eötvös University Budapest,
H-1518, POB 32, Budapest, Hungary

²Air Force Research Laboratory, Materials and Manufacturing Directorate, AFRL/MLLM,
Wright-Patterson Air Force Base, OH 45433, USA

³UES Inc., Dayton, OH 45432, USA

⁴Universal Technology Corporation, Dayton, OH 45432, USA

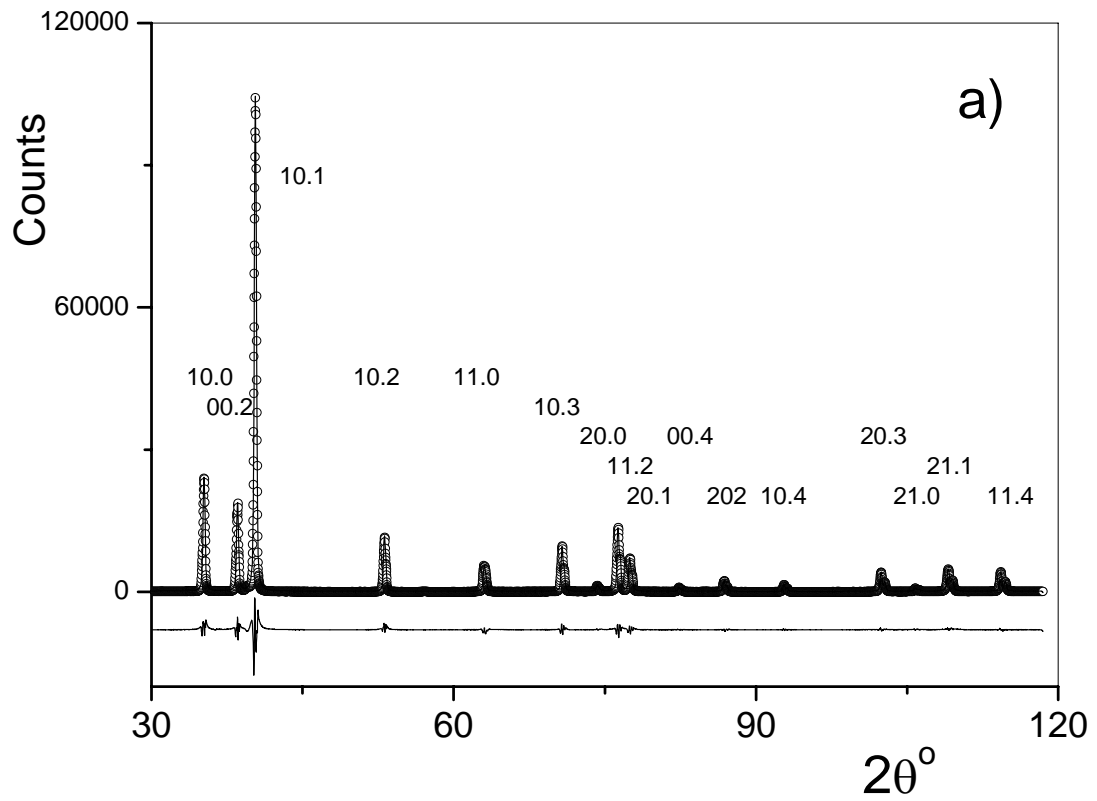
Abstract

High resolution laboratory and special synchrotron X-ray diffraction techniques were used to characterize slip and twinning activity in extruded billets of commercial-purity (CP) titanium. The subgrain size was of the order of a few-hundred nanometers. The laboratory diffraction experiments evaluated the fractions of $\langle a \rangle$, $\langle c \rangle$, and $\langle c+a \rangle$ type dislocations, the average dislocation density (ρ), subgrain size, and the size distribution without twinning. X-ray line profile analysis was used to evaluate stacking faults and twinning assuming $\{10\bar{1}1\}$, $\{11\bar{2}2\}$, and $\{10\bar{1}2\}$ habit planes. Novel synchrotron x-ray diffraction experiments (ESRF synchrotron in Grenoble, France) also enabled the characterization of deformation behavior in individual grains in the polycrystalline CP-Ti, and hence resulted in an accurate description of slip activity.

References

1. T. Ungár, J. Gubicza, A. Borbély, G. Ribárik: Crystallite size-distribution and dislocation structure determined by diffraction profile analysis: Principles and practical application to cubic and hexagonal crystals, *J. Appl. Cryst.* 34. 298-310 (2001)
2. G. Ribárik, T. Ungár, J. Gubicza: MWP-fit: a program for Multiple Whole Profile fitting of diffraction peak profiles by ab-initio theoretical functions, *J. of Applied Cryst.*, 34. 669-676 (2001)
3. G. Ribárik, J. Gubicza, T. Ungár: Correlation between strength and microstructure of ball-milled Al–Mg alloys determined by X-ray diffraction, *Mat. Sci.Eng.* A387–389. 343–347 (2004)
4. T. Ungár, O. Castelnau, G. Ribárik, M. Drakopoulos, J.L. Béchade, T. Chauveau, A. Snigirev, I. Snigireva, C. Schroer and B. Bacroix, Grain to grain slip activity in plastically deformed Zr determined by X-ray microdiffraction line profile analysis, *Acta Materialia*, (2006) *accepted for publication*.

Figure 1. Typical measured (open circles) and fitted (solid line) diffraction pattern, of the measurements made in the Bragg-Brentano (Philips, X'Pert,) diffractometer. (a) Linear intensity scale, (b) logarithmic intensity scale. In the case of the linear scale, pattern (a), the differences between the measured and fitted data are also shown in the bottom of the figure.



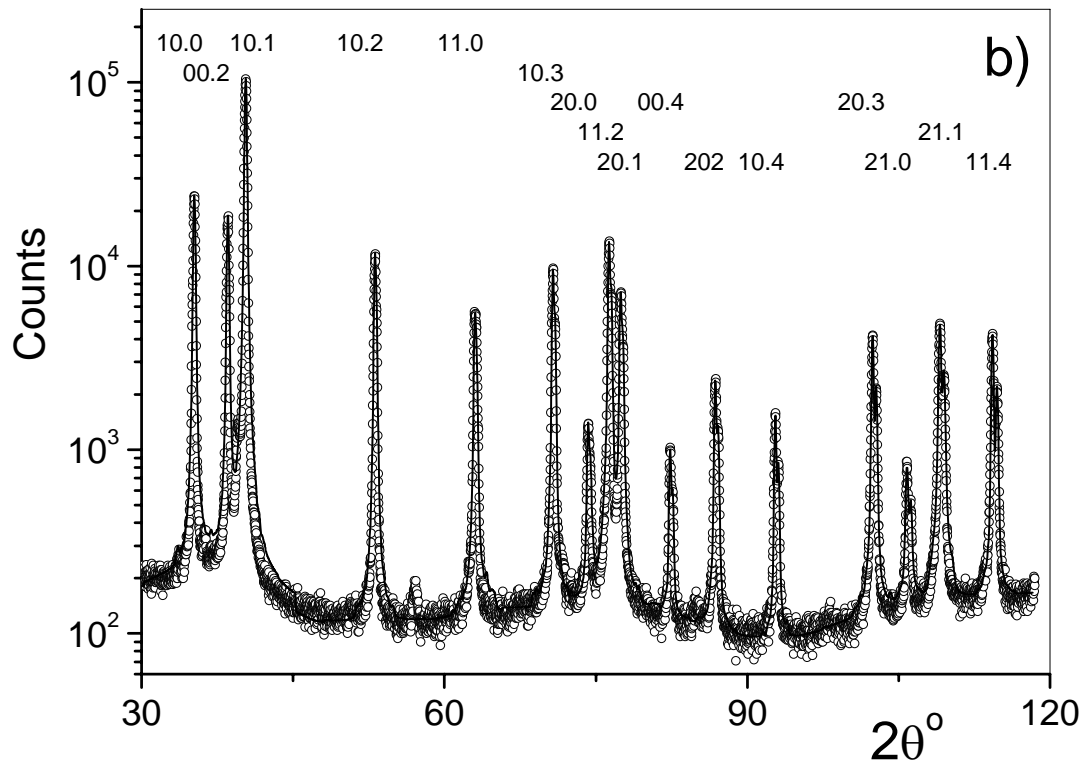


Figure 2. The values of the FWHM in the Williamsol-Hall plot for the initial state specimen. The data were obtained by the high resolution diffractometer using imaging plates (ip) for signal detection. *xx*, *yy* and *zz* indicate the three surfaces of the cube specimen. $K=2\sin\theta/\lambda$, where θ is the diffraction angle and λ the wavelength of X-rays.

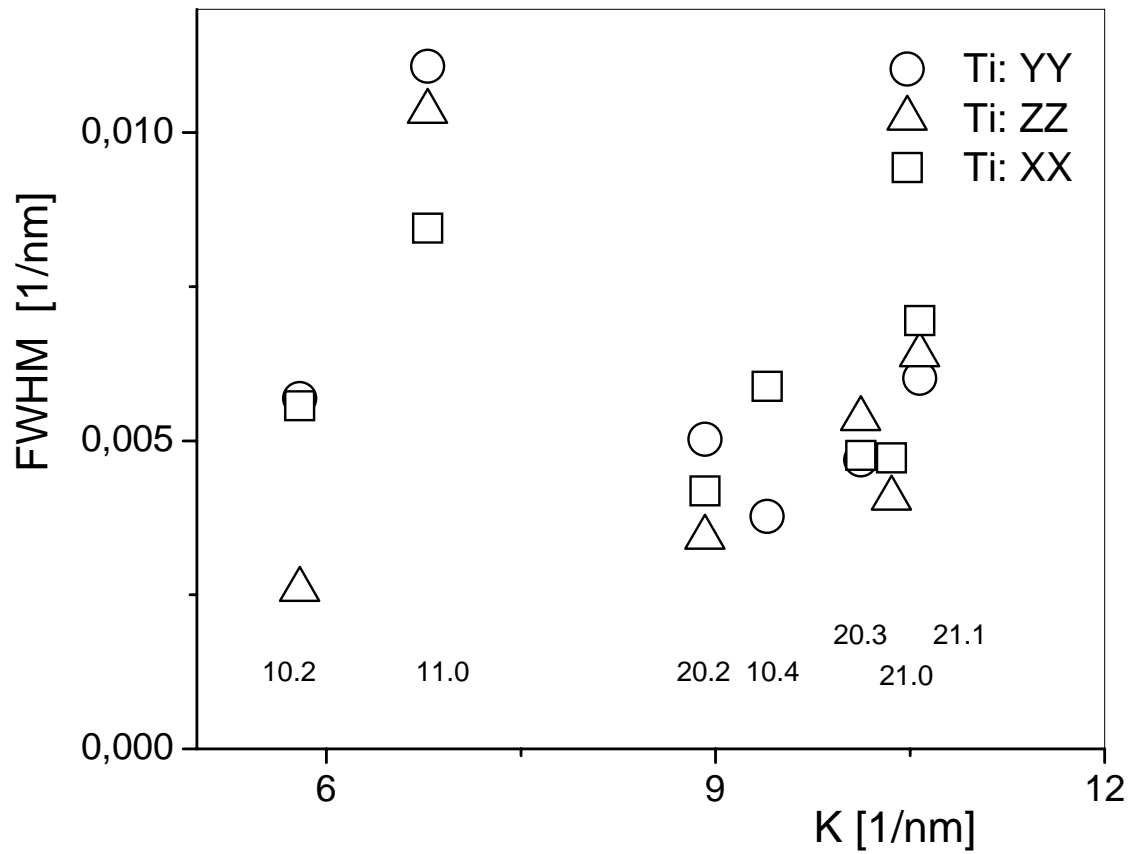


Figure 3. The FWHM values for the three specimens shown in a Williamson-Hall plot as a function of the absolute values of the diffraction vector, $K=2\sin\theta/\lambda$, where θ is the diffraction angle and λ the wavelength of X-rays.

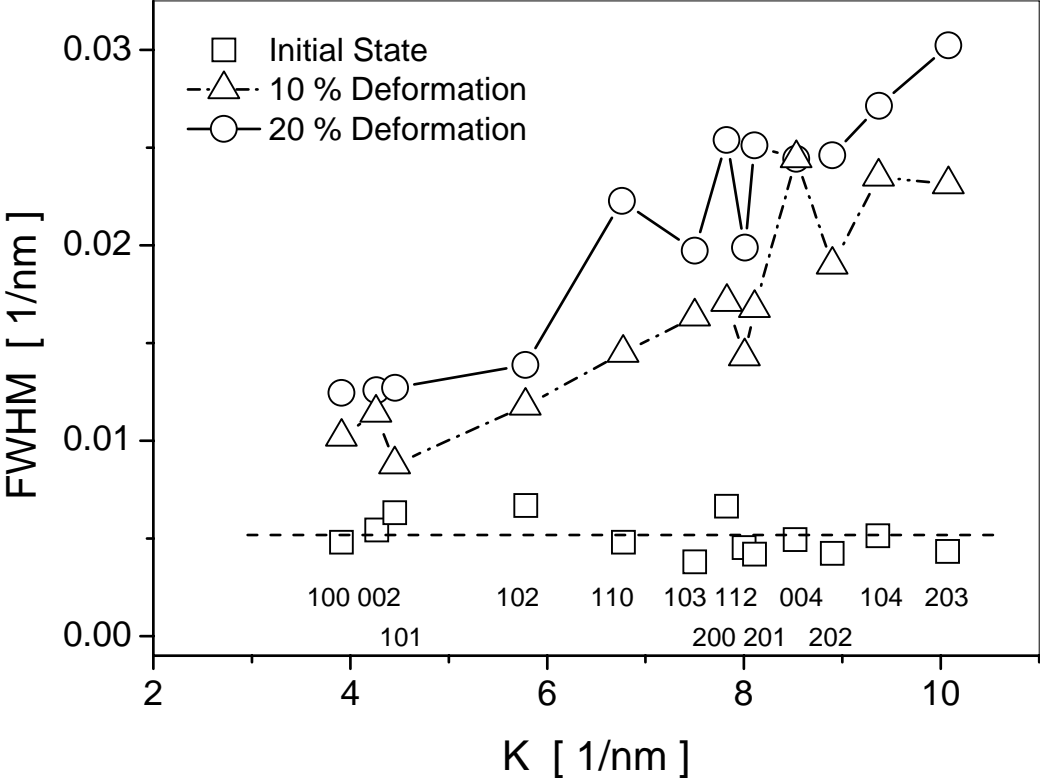
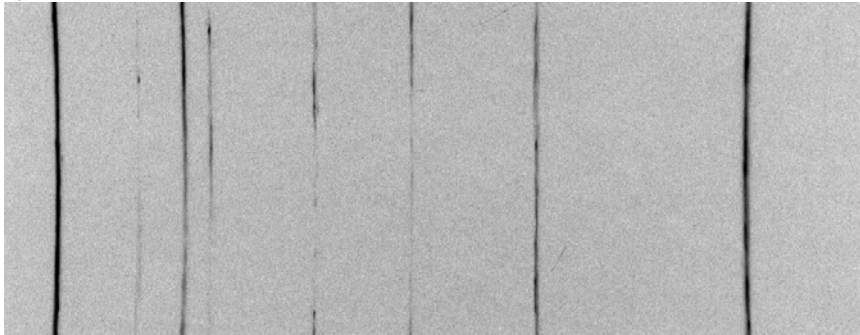


Figure 4. Typical imaging plate (ip) readouts for the initial state (a) and the 20 % deformed (b) specimens in the higher diffraction angle range from about 60 to 120 degrees in 2θ .

a)



b)

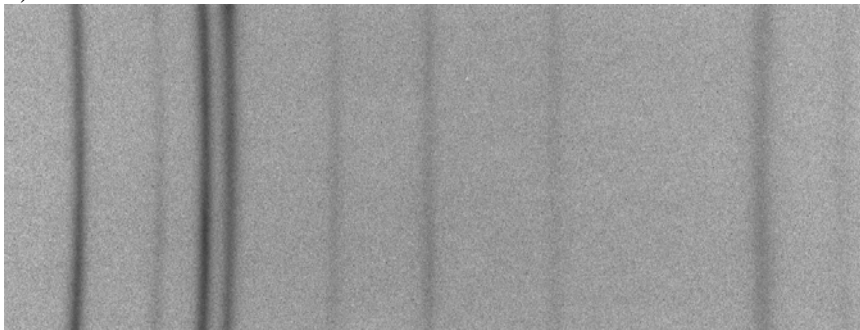
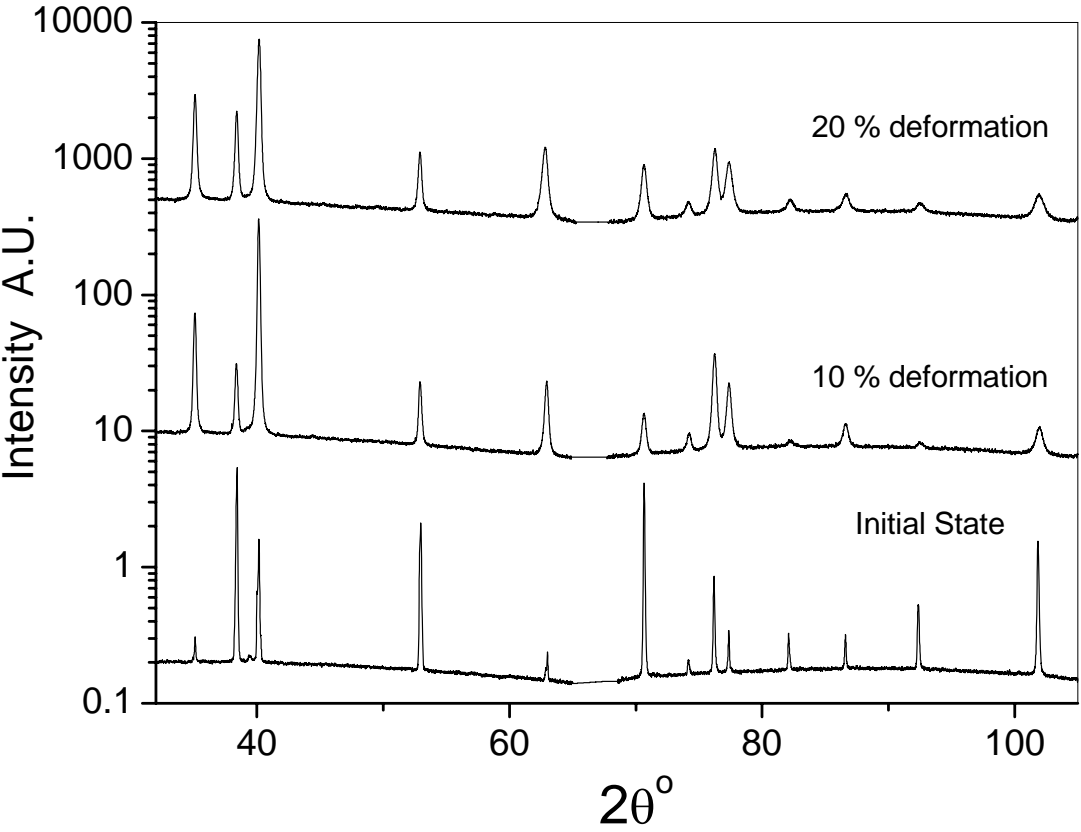


Figure 5. The θ - 2θ diffraction patterns obtained by the correct integration of the intensity along the iso- 2θ lines in the plane of the imaging plates for all three investigated specimens.



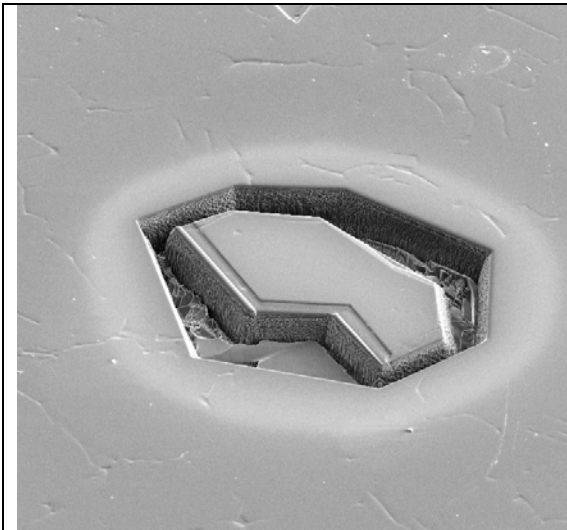


Figure 6a. Scanning electron microscopy (SEM) micrograph of the grain prepared by the method of focused ion beam (FIB) technique. The longer diameter of the grain is about 100 μm .

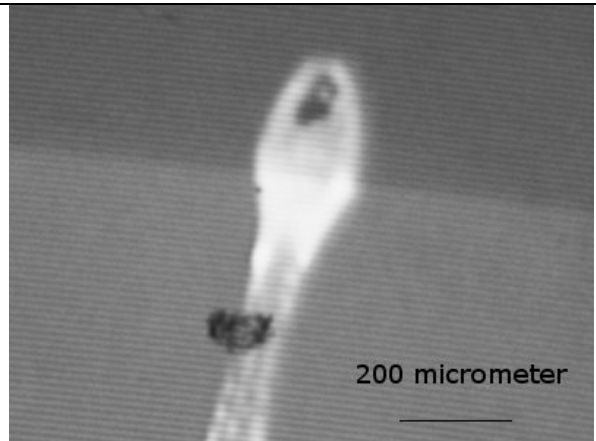


Figure 6b. The grain in Fig. 1 prepared on the tip of a glass fiber. The bulging white spot is the image of the synthetic glue holding the grain, the dark contrast at the upper end of the glue. The glue was selected for not producing any X-ray diffraction effect.

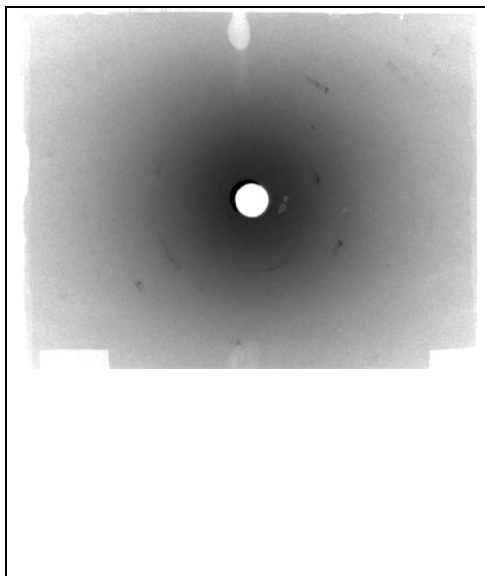


Figure 7a. The Laue micrograph of the single grain. The diffraction spots are weak due to the small size of the specimen.

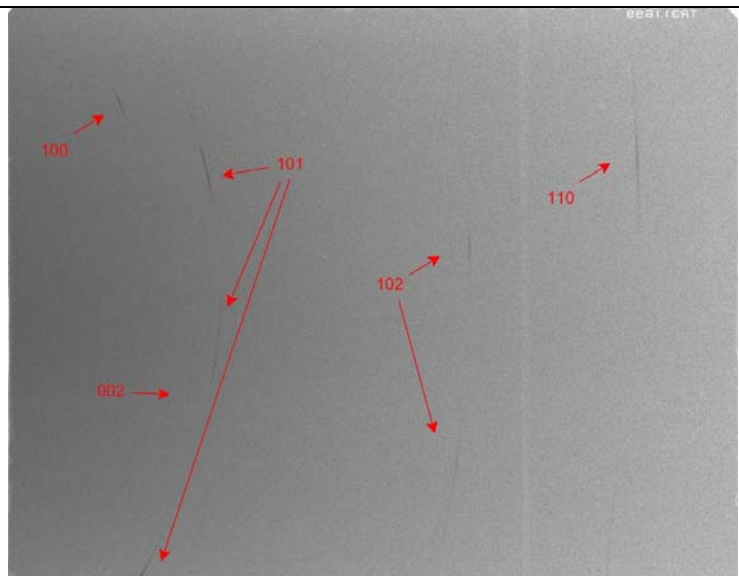
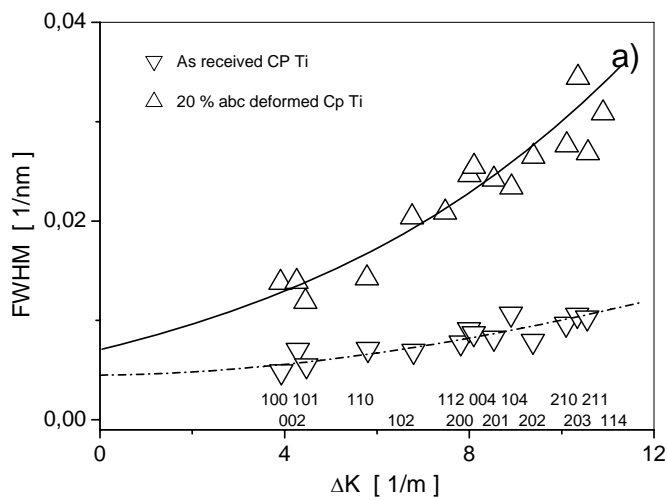
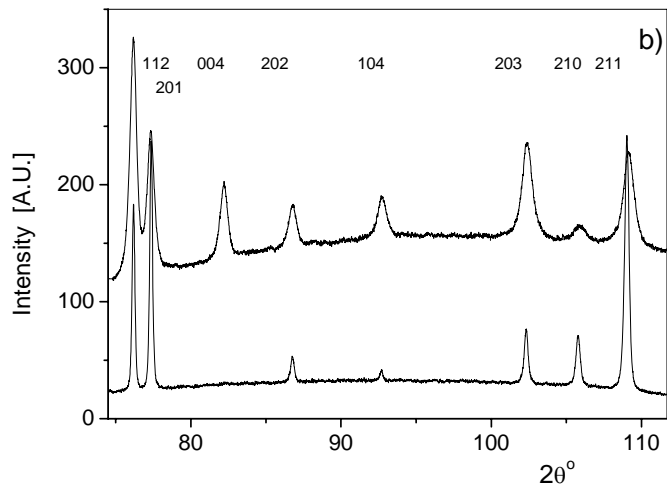
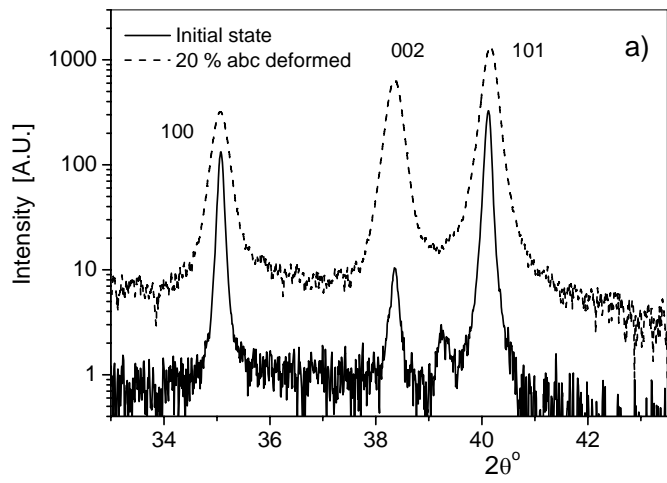
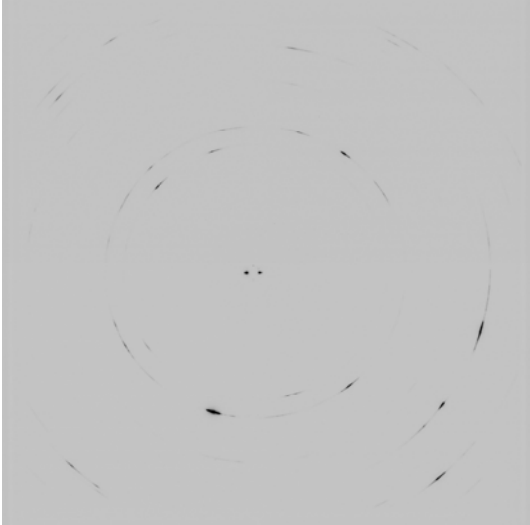
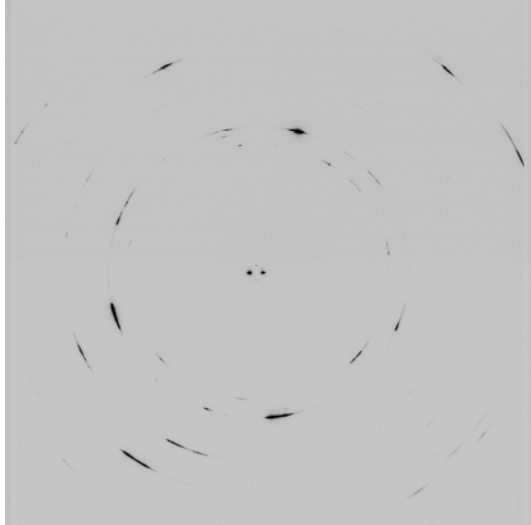
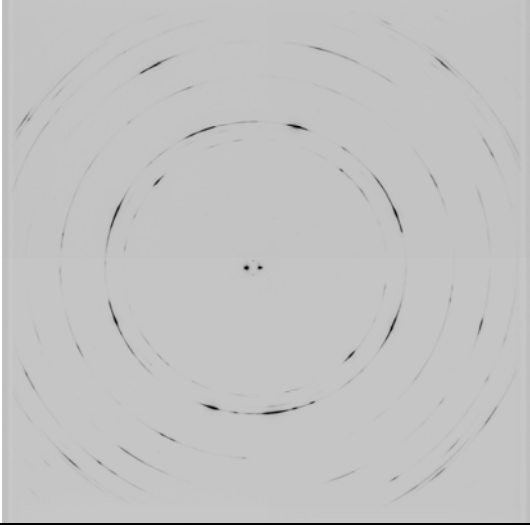
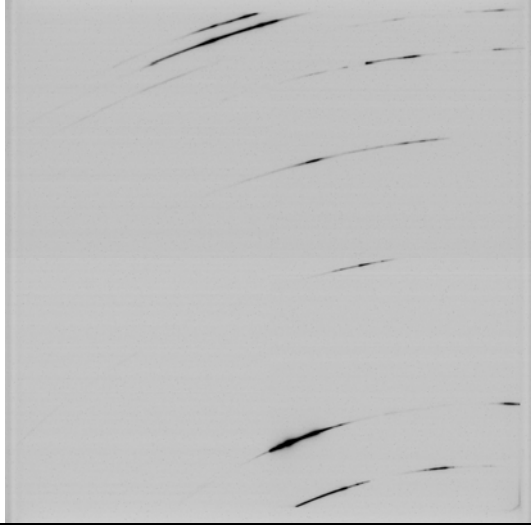


Figure 7b. The imaging plate readout of the diffraction spots corresponding to the grain prepared by the method of FIB. The indices of the different reflections are indicated in red in the figure. It can be seen that there are three 10.1 reflections within about 10 and 15 degrees in the χ direction, while the specimen was rotated over the ω axis by ± 5 degrees. This indicates that the grain definitely consists of more than one crystallite.

Figure 8. Diffraction patterns (a) and (b) and Williamson-Hall plots (c) corresponding to the thin rod specimens measured in the home laboratory.



	
<p>Figure 9a. Typical single frame of the as received CP-Ti specimen in the close detector position, i.e. specimen to detector distance 200 mm.</p>	<p>Figure 9b. Typical single frame of the as received CP-Ti specimen at a different ω setting as compared to the frame in Fig. 7a.</p>
	
<p>Figure 9c. Diffraction pattern after the summation of 300 individual close frames.</p>	<p>Figure 9d. Typical single frame of the as received CP-Ti specimen in the high resolution detector position, i.e. specimen to detector distance 700 mm.</p>